

Study of the precipitation of secondary phases in duplex and superduplex stainless steel

LLORCA-ISERN Núria^{1 a *}, LÓPEZ-JIMÉNEZ Isabel^{1, b}, LÓPEZ-LUQUE Héctor^{1 c}, BIEZMA Maria Victoria^{2 d} and ROCA Antoni^{1 e}.

¹CPCM, Dept. Ciència dels Materials i Enginyeria Metal·lúrgica, Fac. Química, Universitat de Barcelona, Martí-Franquès, 1-11, 08028 Barcelona (Spain)

²Materials Science Department, University of Cantabria, Av. los Castros s/n, 39004 Santander (Spain).

^anullorca@ub.edu, ^bilopezji9@ub.edu, ^chector_10_92@hotmail.com, ^dmaria.biezma@unican.es, ^eroca@ub.edu

Keywords: Duplex and superduplex stainless steel, Microstructure, Sigma and Chi phases, heat treatment, Ageing, carbides and nitrides.

Abstract. The aim of this work is to study the precipitation mechanism of the intermetallic phases present in duplex stainless steels (UNS S32205 and UNS S32750), as well as to find out the most suitable method for detecting and analyzing accurately these secondary phases, particularly Sigma-phase, Chi-phase, nitrides and carbides. The samples were characterized after a solution annealing at 1080°C followed by an isothermal treatment at 830°C from 1 min to 9 h, with the purpose of figuring out the mechanism of chi-phase nucleation and nitrides formation in relation with the sigma-phase. The study has two main objectives: 1) to find out the most suitable technique for the detection, identification and quantification of the secondary phases, obtaining the best results with the combination of field emission scanning electron microscopy (FESEM) and backscattered electron detector (BSE) in comparison with the optical microscopy (MO); 2) to study the influence of the chemical composition on the nucleation mechanism of the intermetallic phases. It has been concluded that molybdenum balance content in chi-phase related to sigma phase is close to two, consequently the kinetics of nucleation and growth of these phases is remarkably faster when this alloying element content in the steel is higher. Chromium nitrides and carbides were also observed to precipitate as a result of the heat treatments carried out to the specimen wherein chromium nitrides role is a favorable site for the nucleation of sigma and chi phases.

Introduction

The microstructure of duplex stainless steels is balanced with 50% austenite (γ) and 50% ferrite (δ) provide to the steel an excellent combination of mechanical and chemical properties. Duplex and superduplex stainless steels possess high strength and corrosion resistance. However, at particular range of temperatures, intermetallic phases, such as sigma phase (σ -phase), chi phase (χ -phase) and chromium nitrides and carbides could precipitate, promoting a matrix impoverishment in critical alloying elements, i.e. chromium, molybdenum and nickel that leads to decrease toughness values and corrosion resistance in these high alloyed steels [1-6]. σ -phase increases the hardness and decreases the toughness as well as the elongation of this type of steels [7] and can change the fracture type from transgranular to intergranular related to increase the σ -phase percentage [8]. χ -phase precipitates as a ternary compound containing Fe, Cr and Mo [9] with a wide range of stoichiometry extending from the ternary χ -phase $\text{Fe}_{36}\text{Cr}_{12}\text{Mo}_{10}$ to $\text{Fe}_{36}\text{Cr}_{12}\text{Mo}_3\text{Ti}_7$ [10] depending on the steel composition. Chi-phase and σ -phase usually are found simultaneously, and this is the main reason to explain the difficulty to study their individual effect on particular properties [10].

Microstructural evolution in these steels has been the scope of previous studies [11–13], but further information is still needed. In this way, this is the main goal of this research: to study microstructural changes, as well as the evolution of mechanical properties in duplex (UNS S32205) and superduplex (UNS 32750) stainless steels plates considering different thermal treatments, with temperature ranges between 600-1000°C, simulating real industrial processes, to enlighten when, where and how the formation of the secondary precipitates takes place inside these steels is necessary in order to prevent potential real problems.

Materials and methods

The materials used were duplex stainless steel grade 2205 (UNS S32205, in this study DSS 2205), and superduplex stainless steel grade 2507 (UNS S32750, in this study SDSS 2507). The chemical composition is shown in Table 1.

Table 1 Chemical composition of DSS 2205 and SDSS 2507 (%wt, balance Fe).

	C	Si	Mn	P	S	Cr	Ni	Mo	N	Cu	Ce
2205	0.015	0.40	1.5	0.018	0.001	22.49	5.77	3.21	0.184	0.18	0.002
2507	0.018	0.26	0.84	0.019	0.001	25.08	6.88	3.82	0.294	0.17	-

The applied thermal treatment was attending the following protocol: a solution-treated at 1080°C for 30 minutes, water quenched, annealing at 830°C, water quench. The aging periods ranged from 1 minute to 9 hours. Metallographic conventional sample preparation has been carried out by grinding and polishing with diamond pastes. Different etching solutions were used including acid-basic reagents as Glyceregia, Grosbeck's, Marble's, Murakami's and Villela's and electrochemical etchings as NaOH and HCl/Ethanol. The microstructural analysis was conducted using an optical microscope Zeiss Axiovert 100 A, and scanning electron microscope FESEM JEOL J-7100F with a coupled Robinson BSE detector. The composition of the different phases was determined using the energy-dispersive X-ray spectroscopy system (EDS) INCA PentaFETx3. In addition, a JEOL JXA-8230 microprobe (with five WDS spectrometers) providing a higher chemical composition accuracy.

Results and discussion

Both optical microscope and FESEM etched specimens observation were performed in order to analyze the microstructural changes experimented by annealed DSS 2205 and SDSS 2507 steels. A recent study explains in deep the most relevant details [2].

Optical microscopy characterization. It is important to point out that were obtained excellent resolution with some etching reagents referred in the literature [14, 15], but others were offered not good performance, therefore were rejected for microstructural characterization (Marble's, Villela's and electrochemical etching with HCl/Ethanol).

Glyceregia reagent provides the best contrast between ferrite phase and σ -phase, but the etching time step, close to 2 minutes, could be considered too high in particular cases. Grosbeck's reagent has the advantage of differentiating nitrides (darkest phase), but requires an imprecise time of etching (1-10 minutes). Between the different chemical etching reagents, Murakami reagent was found to be the most convenient due to its short time of etching and sufficient contrast between the different phases. However, it is difficult to identify ferrite phase when present in small percentages, this similar behaviour is presented with the option of electrochemical etching with a 20% NaOH.

Scanning electron microscopy characterization. FESEM was also used based in previous studies [13, 14]. Unfortunately, the results were unsatisfactory due to the formation of oxide layers (Fig. 1A). Some phase boundaries are initially dissolved and could disappear any phase depending

on the nucleation side as consequence of etching. Therefore, unetched samples were imaged in the FESEM and back-scattered electron (BSE) detector. Since σ -phase and specially χ -phase contain higher percentage of molybdenum, their contrast is enhanced compared to that of ferrite and austenite. In Figure 1B, the different phases can be clearly identified. The dark spots are identified as carbide and nitrides and FE-SEM-BSE coupled system is the best combination to study secondary phases in DSS and SDSS.

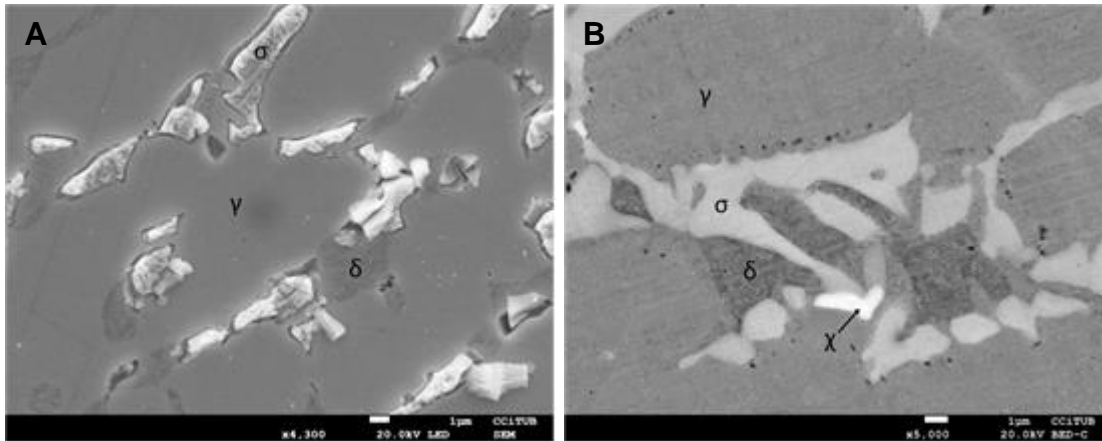


Figure 1. FESEM-BSE image of DSS 2205 aged 1 hour at 830°C A) etched with NaOH B) unetched sample

The energy-dispersive X-ray spectroscopy (EDS) obtained for DSS 2205 and SDSS 2507 showed that early phases are austenite and ferrite which higher relative percentage of nickel and chromium respectively. The intermetallic phases started to nucleate after the samples were heat treated between 1 and 5 minutes: σ -phase, rich in chromium and molybdenum, and χ -phase with a remarkably higher content in molybdenum than any other phase in these steels and a similar content in chromium to ferrite phase. These compositional values are in agreement with previous studies [1, 4, 12, 13]. The first important microstructural change was related to the precipitation of small dark grey and black spots in annealed samples during times lesser than 3 minutes (Fig. 2).

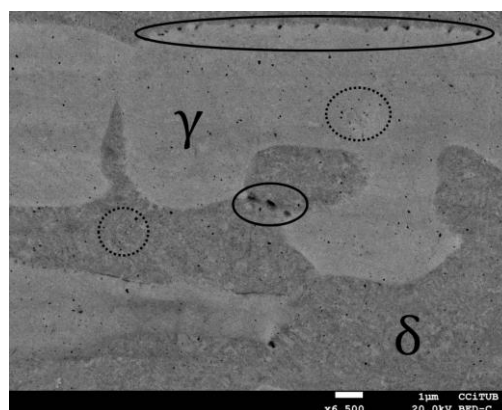


Figure 2. DSS 2205 3 minutes. Chromium nitrides (solid circles). Carbides (dotted circles).

Wavelength-dispersive spectroscopy (WDS) of these samples showed an accumulation of chromium nitrides in the dark gray particles. Its nucleation is at ferrite/ferrite and austenite/ferrite boundaries, and also at ferrite/ferrite/ferrite triple points. This precipitation is driven by a high cooling rate as a result of accommodating substantial amounts of nitrogen in ferrite supersaturated solid solution, as previously reported by Nilsson and Wilson [1]. The other dark phases are carbides,

distributed mainly intragranularly and heterogeneously all over the austenite and ferrite phases as dark spots in the form of globular particles.

Phase analysis in duplex and superduplex stainless steel. Both σ -phase and χ -phase start their fast nucleation process after initial ageing treatment and as result of precipitation of nitrides and carbides (ranging from 3 to 5 minutes 1 and 3 minutes for DSS 2205 and SDSS 2507). Strong ferrite stabilizers addition into the stainless steels (Cr, Si or Mo) rapidly leads to the formation of the intermetallic phases [16]. σ -phase and χ -phase have a combined growth step, although the amount of χ -phase is certainly higher at the beginning of the process since the apparent inability of σ -phase to nucleate at ferrite/ferrite boundaries without a previously precipitated χ -phase or chromium nitrides at identical position. It could be due to the ferrite stabilizers diffusion values at low time treatments, which might cause a higher local supersaturation that leads χ -phase nucleation, instead of the nucleation of σ -phase. On the other hand, our results show that both phases were found at ferrite/ferrite/austenite triple points and ferrite/austenite boundaries, nucleating at the phase boundary in the highly chromium concentrated region of ferrite with a hemispheric morphology, which were observed to only grow towards ferrite phase.

Chromium nitrides, which precipitate before σ -phase and χ -phase, act as a favorable site for the nucleation of the new intermetallic phases. Chromium nitrides precipitating at ferrite/austenite boundaries and at triple ferrite/ferrite/ferrite points act as a site of nucleation for σ and χ phases. Figure 3A shows an example of the microstructural features for the studied DSS and SDSS for the described thermal treatment pointing out the location of chromium nitrides. The long-time treated samples showed a less interconnected distribution of nitrides as a result of the growth of σ -phase and χ -phase, as reported by Breda et al. [17]. As a result of the formation of σ -phase and secondary austenite, the boundaries between the different phases are blurred, losing the originally banded morphology (Fig. 3B).

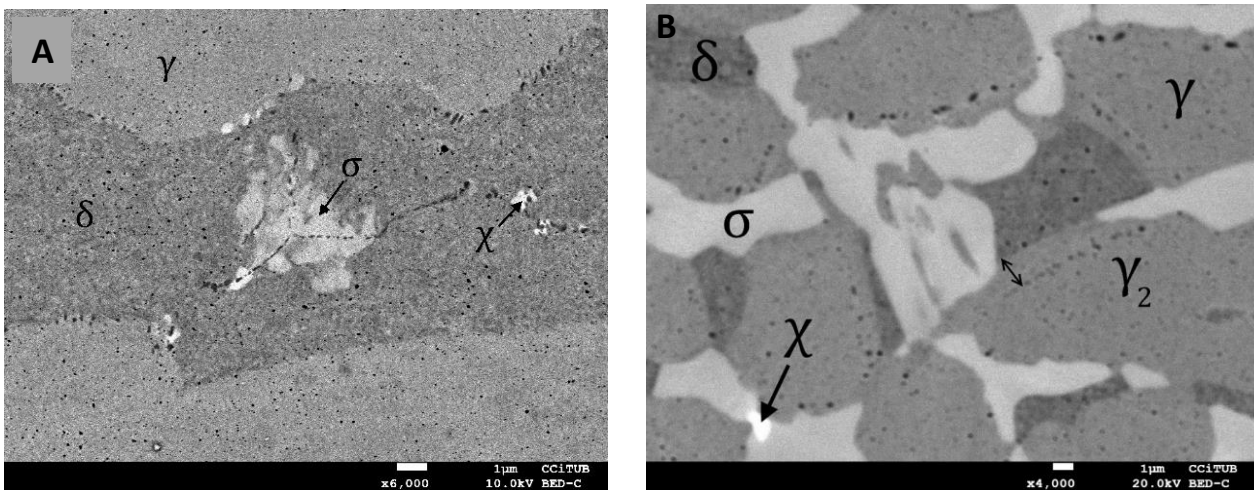


Figure 3. DSS treatment at 830°C for: A) 5 minutes B) 9 hours.

Final σ -phase shape is somehow blunted compared to the starting ferrite morphology, caused by the linking between single sigma crystals. Consequently, austenite phase shows an enlargement in relation to the specimen without thermal treatment. Simultaneously to the enrichment in chromium and molybdenum of σ -phase and χ -phase during their propagation process, nickel diffuses into ferrite. The enrichment of austenite stabilizing elements in ferrite and the loss of ferrite stabilizing elements, leads to an unstable ferrite that transforms into secondary austenite [11]. EDS-Linescan microanalyses were performed in order to better understand the relationship between composition and microstructure. Figure 4 shows an example of DSS treated for 1 hour, which confirms the above

presented hypothesis: nickel gathers smoothly in austenite, iron content decreases in the intermetallic phases, chromium and molybdenum content increases considerably in σ -phase and χ -phase respectively, although a lower but remarkable peak can also be noticed in σ -phase for molybdenum.

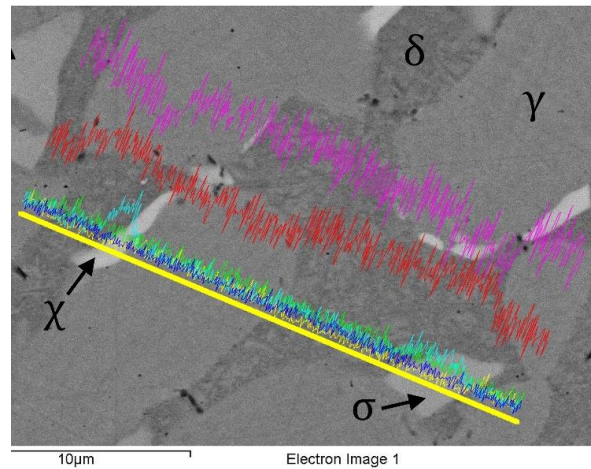


Figure 4. Linescan microanalysis of DSS 2205 830°C for 1 hour. Distribution of: iron (purple line), chromium (red line), nickel (yellow line), molybdenum (pale blue line), manganese (green line) and oxygen (dark blue line).

Conclusions

The microstructural changes in plated-shape duplex stainless steel UNS S32205 and in superduplex stainless steel UNS S32750 at different thermal treatments has been investigated, pointing out that Murakami's reagent and NaOH electrolytic etching are the best OM options and combination of FESEM-BSE microscopy on unetched samples offers by far the best accurate and precise phases detection and differentiation. Moreover, all the phases, even the Chi-phase, nitrides and carbides, in small amount, were clearly identified without using crystallographic analysis.

The progress of the nucleation and growth of secondary phases can be stated as follows: chromium nitrides and carbides, χ -phase (phase with the highest content in molybdenum) and finally σ -phase. Chromium nitrides act as a favorable site for the nucleation of χ -phase, and both of them then encourage the formation of σ -phase. However, the growth of the chromium nitrides and χ -phase slows down earlier than the growth of σ -phase itself. χ -phase content decreases as more σ -phase is formed, whereas the chromium nitrides remain stable through treatment time and their location is kept from their original nucleation site.

The kinetics of the transformations is related to the composition and specimens thermomechanical history: in SDSS 2750, the σ -phase completely replaces ferrite phase, whereas same thermal treatment conditions the ferritic phase still remains with relevant percentages in DSS 2205. All these "new" phases nucleating in both duplex and superduplex steels appeared at very short heat treatment time, and unlike the carbides, they all precipitated at grain boundaries, which suggest that it is advisable to avoid employing these steels at this temperature range.

References

- [1] J. O. Nilsson, A. Wilson, Influence of isothermal phase transformations on toughness and pitting corrosion of super duplex stainless steel SAF 2507, *J. Mater. Sci. Technol.* 9 (1993) 545-554.
- [2] N. Llorca-Isern, H. López-Luque, I. López-Jiménez, M. V. Biezma, Identification of sigma and

chi phases in duplex stainless steels, *Mater. Charact.* 112 (2016) 20-29.

- [3] S. Bernhardsson, The corrosion resistance of duplex stainless steels, *Duplex Stainless Steels'91*, 1 (1991) 185–210.
- [4] T. Chen, K. Weng, J. Yang, The effect of high-temperature exposure on the microstructural stability and toughness property in a 2205 duplex stainless steel, *Mater. Sci. Eng., A.* 338 (2002) 259-270.
- [5] H. Sieurim, R. Sandström, Sigma phase precipitation in duplex stainless steel 2205, *Mater. Sci. Eng., A.* 444 (2007) 271-276.
- [6] A. F. Padilha, C. F. Tavares, M. A. Martorano, Delta Ferrite Formation in Austenitic Stainless Steel Castings, *Mater. Sci. Forum.* 730-732 (2012) 733-738.
- [7] I. K. JooSuk LEE, Application of Small Punch Test to Evaluate Sigma-Phase Embrittlement of Pressure Vessel Cladding Material, *J. Nucl. Sci. Technol.* 40 (2003) 664–671.
- [8] M. V. Biezma, C. Berlanga, G. Argandona, Relationship between microstructure and fracture types in a UNS S32205 duplex stainless steel, *Mater. Res.* 16 (2013) 965-969.
- [9] Y. H. Lee, K. T. Kim, Y. D. Lee K. Y. Kim, Effects of W substitution on ζ and χ phase precipitation and toughness in duplex stainless steels, *Mater. Sci. Technol.* 14 (1998) 757-764.
- [10] R. Gunn, *Duplex stainless steels: microstructure, properties and applications.* Elsevier, New York, 1997.
- [11] O. S. Michael Pohl, Effect of intermetallic precipitations on the properties of duplex stainless steel, *Mater. Charact.*, no. 1, pp. 65–71, 2007.
- [12] S. K. Ghosh, S. Mondal, High temperature ageing behaviour of a duplex stainless steel, *Mater. Charact.*, 59 (2008) 1776-1783.
- [13] D. M. Escriba, E. Materna-Morris, R. L. Plaut, A. F. Padilha, Chi-phase precipitation in a duplex stainless steel, *Mater. Charact.* 60 (2009) 1214-1219.
- [14] J. Michalska, M. Sozańska, Qualitative and quantitative analysis of σ and χ phases in 2205 duplex stainless steel, *Mater. Charact.* 56 (2006) 355-362.
- [15] G. F. V. Voort, *Metallography, Principles and Practice.* ASM International, Materials Park, OH, 1984.
- [16] C.-C. Hsieh, W. Wu, Overview of Intermetallic Sigma Phase Precipitation in Stainless Steels, *ISRN Metallurgy*, 2012 (2012) 1-16.
- [17] M. Breda, M. Pellizzari, M. Frigo, σ -Phase in Lean Duplex Stainless Steel Sheets, *Acta Metall. Sin. (Engl. Lett.)*, 28 (2015) 331-337.